Emergency rate-driven control for rotor angle instability in power systems

Cite as: Chaos **32**, 061102 (2022); https://doi.org/10.1063/5.0093450
Submitted: 29 March 2022 • Accepted: 09 May 2022 • Published Online: 01 June 2022

Suchithra K. S., Gopalakrishnan E. A., Jürgen Kurths, et al.

Emergency rate-driven control for rotor angle instability in power systems

Cite as: Chaos **32**, 061102 (2022); doi: 10.1063/5.0093450
Submitted: 29 March 2022 · Accepted: 9 May 2022 ·
Published Online: 1 June 2022

Suchithra K. S.,[1] Gopalakrishnan E. A.,[2,a)] Jürgen Kurths,[3,4] and E. Surovyatkina[4,5]

AFFILIATIONS

[1]Department of Electrical & Electronics Engineering, Amrita School of Engineering, Amrita Vishwa Vidyapeetham, Coimbatore 641112, India
[2]Center for Computational Engineering and Networking (CEN), Amrita School of Engineering, Amrita Vishwa Vidyapeetham, Coimbatore 641112, India
[3]Department of Physics, Humboldt University of Berlin, Newtonstrasse 15, Berlin 12489, Germany
[4]Potsdam Institute for Climate Impact Research, Potsdam 14412, Germany
[5]Space Research Institute of Russian Academy of Sciences, Moscow 117997, Russia

[a)]**Author to whom correspondence should be addressed:** ea_gopalakrishnan@cb.amrita.edu

ABSTRACT

Renewable energy sources in modern power systems pose a serious challenge to the power system stability in the presence of stochastic fluctuations. Many efforts have been made to assess power system stability from the viewpoint of the bifurcation theory. However, these studies have not covered the dynamic evolution of renewable energy integrated, non-autonomous power systems. Here, we numerically explore the transition phenomena exhibited by a non-autonomous stochastic bi-stable power system oscillator model. We use additive white Gaussian noise to model the stochasticity in power systems. We observe that the delay in the transition observed for the variation of mechanical power as a function of time shows significant variations in the presence of noise. We identify that if the angular velocity approaches the noise floor before crossing the unstable manifold, the rate at which the parameter evolves has no control over the transition characteristics. In such cases, the response of the system is purely controlled by the noise, and the system undergoes noise-induced transitions to limit-cycle oscillations. Furthermore, we employ an emergency control strategy to maintain the stable non-oscillatory state once the system has crossed the quasi-static bifurcation point. We demonstrate an effective control strategy that opens a possibility of maintaining the stability of electric utility that operates near the physical limits.

The recent paradigm shift in integrating intermittent renewable energy (RE) and plug-in electric vehicles has increased uncertainties in power systems. These uncertainties alter the operational schedule and stability margin of the system. Therefore, there is significant research interest in power system dynamics in the presence of uncertain fluctuations. Studies on the impact of fluctuations hitherto are based on the approximation of the system as autonomous. In this work, we investigate the effect of noise on the power system transition characteristics for different operating environments, preserving the non-autonomous behavior of the system. We also propose a control strategy for the power system model considered. Considering power system operation close to the physical limits and the chances of cascading failures affecting major sectors of the society, a control strategy which allows one to regain the stability is highly pertinent.

I. INTRODUCTION

Power networks are undergoing a fundamental transition to tap abundant and cost-free renewable energy sources (RESs) as promising alternatives to conventional, limited supply energy sources. The integration of renewable energy, which is intermittent in nature, brings in significant uncertainty and fluctuations in the power generation.[1] The increased uncertainties and fluctuations alter the operational schedule[2] and stability margin[3] of the power system. Therefore, we need to investigate the power system dynamics under uncertainties and fluctuations.[4–8] Power systems with uncertainties are modeled as stochastic systems by modeling the uncertainties as noise. Hence, power systems dynamics are described by stochastic nonlinear differential equations.[1] Stochastic nonlinear systems are found to exhibit novel dynamical features[9,10] and transitions[11] that are absent in the deterministic counterparts.

The diverse manifestation of noise demands a thorough investigation and characterization of the dynamics of stochastic power systems to ensure reliable operation.

The uncertainty levels in modern power systems, including wind and solar sources, are so high as to trigger a critical transition (CT), leading to collapse.[12] The transient stability assessment of a stochastic power system is challenging due to the cumulative effects of the random transient disturbances and uncertainties.[13] The customary practice in power systems to analyze the transient stability under stochastic disturbances is to adopt canonical models that retain the essential features for the analysis.[14] The commonly used canonical model is a single infinite machine bus (SMIB), in which a single generator is connected to an infinite bus.[15–17] The widely accepted methodologies to address the transient stability of a stochastic power system are probabilistic approaches[18] and time-domain simulations.[19]

Odun-Ayo and Crow[20] presented a quantitative measure of the probability of stability suitable for transient disturbances using stochastic Lyapunov methods. Furthermore, Wang and Crow[16] analyzed transient stability of stochastic SMIB by investigating qualitative changes occurring in the corresponding probability density function (Pdf). The authors determined the evolution of Pdf over time with Fokker Planck equations. A successive study by Ju *et al.*[1] computed the stability probability by evaluating the energy function, which is further analytically solved using stochastic averaging.

Shahidehpour and Qiu performed one of the pioneering works of transient stability of a stochastic power system using the Langevin equation of motion.[4] The authors formulated a stability measure for the SMIB power system model based on the mean exit time from the time-domain simulations. After that, Marco and Bergen[15] adopted a structure-preserved, single generator-single load power system model and developed a stability measure based on the mean exit time from the domain of attraction of SEP for voltage collapse. These studies on the canonical model help one to assess transient stability based on the mean first exit time from the domain of attraction of the stable equilibrium point (SEP) as a function of the magnitude of perturbations.[4,15]

Furthermore, Dhople *et al.*[21] analyzed the transient stability of a stochastic power system through a linear stability analysis. They illustrated the formulation of a stochastic hybrid system from the linearized system to compute the moments of the state variable to assess the transient stability. Most of the transient stability studies performed on stochastic power systems examined the exit time/moments of the state variable from the domain of attraction of SEP. However, these studies do not give information about the available operation margin in the parameter space. In order to evaluate the available operating margin in the parametric space, Wang and Crow[22] performed a transient stability analysis of a stochastic power system from the perspective of the bifurcation theory. The study on a three machine nine bus stochastic power system model illustrated a singularity induced bifurcation near the point of voltage instability in the parameter space in the presence of random fluctuations.

In summary, the literature covered until now analyzed the transient stability of stochastic power systems using canonical models. A significant amount of literature reported the impacts of the intensity of stochastic fluctuations on the stability of power systems from the viewpoint of bifurcation theory. However, these studies examined the quasi-static variation of the bifurcation parameter in an autonomous power system model. The studies on other dynamical systems confirm that stability regimes in autonomous and non-autonomous systems are different.[23,24] Therefore, it is essential to consider the time evolution of the system parameters for the stability analysis to get a correct picture of the stability regimes of stochastic power systems. Hence, we focus on the numerical time-domain simulations of non-autonomous stochastic power systems in this work.

Suchithra *et al.* reported the first study on the delay in the point of transition to the alternate state in a bi-stable power system model for the variation of system parameter as a function of time.[25] Furthermore, the authors reported an early transition to the undesirable alternate state when the mechanical power is varied as a function of time in a deterministic power system model.[26] In this study,[26] they proved that the stable branch ceases to exist beyond the quasi-static bifurcation point, which leads to completely different behavior in comparison with the case when the stable branch becomes unstable.[27] They also demonstrated a relationship between the initial conditions and the rate of evolution of the bifurcation parameter that triggers a transition to the undesirable state. In this paper, we numerically examine the effect of various noise intensities in a non-autonomous bi-stable power system oscillator model. We determine the relationship between the speed at which the system parameters vary and the fluctuation intensity at the generation side. Furthermore, we propose a rate-driven control to reverse the system to the stable non-oscillatory state even after crossing the bifurcation point. The results obtained via this approach help us to maintain the stability when significant levels of stochastic fluctuations are present.

The organization of the paper is as follows. Section II describes the stochastic power system model employed for our investigation. Section III presents the stochastic system response under the variation of mechanical power as a function of time, followed by the rate-driven control strategy, which enables smooth reversal of the transition from the emergent state. Finally, the conclusions are presented in Sec. IV.

II. STOCHASTIC POWER SYSTEM MODEL

We consider the canonical SMIB power system model, widely adopted to study transient electromechanical dynamics, for our investigation. The governing dynamics of the system are explained with a three degree of freedom (DOF) swing equation that incorporates the effects of flux decay. Flux decay plays a significant role in angular instability.[28,29] The synchronous machine transforms the mechanical power input, P_m, to the electrical power output, P_e. The governing dynamics are described as follows:

$$M\ddot{\delta} + D\dot{\delta} = P_m - P_e, \tag{1}$$

$$P_e = \frac{EV\sin(\delta)}{x'_d\Sigma}, \tag{2}$$

$$T_{d0}\dot{E} = E_f - \frac{E(x'_d\Sigma + (x_d - x'_d)) + V\sin\delta}{x'_d\Sigma}. \tag{3}$$

Here, M and D represent the inertia and the damping constant; δ is the displacement of the rotor angle with respect to the synchronous

frame; E is the induced electromotive force (emf), which is given by Eq. (3), and V is the voltage at the infinite bus; E_f denotes the excitation voltage to the field winding; $x'_d\Sigma$ denote the lumped reactance of the synchronous machine and transmission line. x_d and x'_d, respectively, represent the direct axis reactance in steady and transient states. The direct axis open-circuit time constant is denoted by T_{d0}. The time derivative of δ is denoted as ω, which denotes the difference in the angular velocity from the synchronous reference frame. We use the normalized equations as in Kundur[14] and make the following substitutions for convenience:

$$b = \frac{EV}{XM}, \quad \gamma = \frac{D}{M}, \quad X' = x_d - x'_d, \quad B = \frac{1}{x'_d\Sigma}.$$

The difference between the two reactances, X' denotes the effective reactance of the system. Furthermore, we fix the standard values to the parameters in the governing equation as given below:[28,29]

$$M = 0.3, \quad D = 0.2, \quad T_{d0} = 2, \quad X' = 1, \quad E_f = 1, \quad B = 1.$$

We have shown the inception of limit cycle oscillations and a sub-critical Hopf bifurcation in the same power system model.[26] The model also captures many dynamical features such as period-doubling oscillations and chaos[28] in various parameter regimes.

We focus on the perturbations due to stochastic variations of generation. The intermittent feed-in from wind and solar generations are modeled as α-stable Lèvy type noise[30,31] in the literature.[30,31] However, we apply additive white Gaussian noise (AWGN) as a first approximation. The conventional practice in power systems is to choose white Gaussian noise to model stochasticity in power systems occurring at the generation side, where the power system is represented as SMIB.[16,17] In our study, we analyze the effect of the dynamic evolution of system parameters in the presence of AWGN of varying intensities. AWGN is generated by a Wiener process, as in the literature.[16,32] The properties of the Wiener process are available in the literature.[19] The SMIB with AWGN is given below:

$$d\delta = \omega\, dt, \tag{4}$$

$$d\omega = \left(P_m - \frac{EV}{X}\sin\delta - D\omega\right) dt + \beta\, dW(t), \tag{5}$$

$$T_{d0} dE = E_f - E(1+X) + V\cos\delta + \beta\, dW(t), \tag{6}$$

where $\beta W(t)$ are the stochastic continuous disturbances, $W(t)$ represents the Wiener process, and β is the noise intensity. Wang *et al.*[16] investigated the effects of AWGN on the stability regimes of SMIB by tracing the evolution of Pdf of the dynamic trajectories. However, the effect of AWGN when the system parameters change as a function of time is not explored. Ours is the first numerical study that focuses on the influence of noise on the transition characteristics for the variation of system parameters as a function of time. We employ stochastic Runge–Kutta method with a step size of 0.01 for the numerical integration.[33]

III. RESULTS

A. Transitions in the power system model for the mechanical power variations as a function of time in the presence of fluctuations

In this section, we evaluate the response of the system for variation of system parameters as a function of time in the stochastic bi-stable power system oscillator. Even though the stability of a bi-stable power system oscillator is well investigated, these studies focus on the static bifurcation analysis of the bi-stable oscillator.[28,34] Perpetual changes in load and generation associated with RES make modern power systems non-autonomous.[35] In our earlier work, we have established that the system continues to hover around the stable equilibrium point for a slow variation of the system parameter. Hence, the onset of oscillations is delayed with respect to the quasi-static bifurcation diagram.[25] To be specific, the destabilization of the slowly varying trajectory does not occur immediately upon crossing the bifurcation point, determined by a quasi-static bifurcation analysis.[23]

Here, we inspect the influence of stochasticity in the bi-stable power system model, where the system parameter varies as a function of time. The mechanical power varies as a function of time, as in the previous study,[25] as follows:

$$P_m(t) = P_{m0} + \mu t, \tag{7}$$

where P_{m0} is the initial value of the mechanical power and μ is the rate at which mechanical power is varied. We allow a linear evolution of mechanical power as discussed in the literature.[36] We have paid sufficient attention to eliminate the possibility of severe transient disturbances by limiting the maximum rate at which the bifurcation parameter evolves, which is beyond the scope of this work. In our experiments, we have non-dimensionalized noise before performing the experiment as in the literature.[37]

We capture the time series of the state variable ω for the investigation, which contains sufficient information about the state of the power system.[38,39] In order to investigate the response of the system to variations in initial conditions, we consider two sets of initial conditions, one at a finite distance from the fixed point and the second close to the fixed point. We fix the initial value of ω at $\omega_0 = 1.5$ for the first set of experiments. Here, we vary P_m from 0.3 to 0.9 in the presence of a non-dimensionalized noise intensity of 3% in the system. A non-dimensionalized noise intensity of 3% means that the ratio of the RMS value of the angular velocity at the applied noise level is 3% to the RMS value of limit cycle oscillations in the absence of noise. For clarity, we denote the non-dimensional noise intensity as σ. As time evolves, the system parameter P_m is varied at predefined fixed rates as in Eq. (7). We considered three different rates for our investigation as in the literature.[40] The three different rates considered for the study are $\mu_3 = 0.0001$, $\mu_2 = 0.0002$, and $\mu_1 = 0.0003$. The trajectories are plotted against the quasi-static bifurcation diagram to distinguish the effects of rate and noise. In order to plot the quasi-static bifurcation diagram, we increase the non-dimensional mechanical power, P_m, in a quasi-static manner, keeping the initial conditions constant. We record the root mean square (RMS) value of the angular velocity for each P_m. An oscillatory response and sudden increase in the magnitude of ω are obtained when the mechanical power crosses the first critical value,

P_{mCT1}. Furthermore, we change the initial conditions of the system and decrement P_m to get the second critical value (P_{mCT2}), wherein we observe the reverse transition from the oscillatory state to the stable fixed point. Figure 1(a) presents the transitions for the variation of mechanical power as a function of time, $\omega(t)$ of the canonical power system model for different rates of evolution of system parameters corresponding to $\omega_0 = 1.5$.

We notice an effect of the early crossing of the unstable manifold for higher rates of variation of mechanical power, irrespective of the initial P_{m0} value. Specifically, the point at which the system crosses the unstable manifold while nearing the Hopf point is dependent upon the rate at which P_m evolves. As a result, for systems with higher μ, the system crosses the unstable manifold and gets attracted to the stable limit cycle at a lower value of P_m.

Next, we repeat the experiment for the same rate of evolution of the system parameters as earlier, except for a different initial condition, when $\omega_0 = 0.1$. We observe that the dynamic trajectories, $\omega(t)$ crossover the unstable manifold without maintaining a specific trend in the rates in Fig. 1(b), quite different from Fig. 1(a). Then, to analyze the reason behind the different order of crossing the unstable manifold, we closely inspect the dynamic trajectories near the bifurcation point. We identify that the order in which the system crosses the unstable manifold is greatly determined by external stochastic excitation for the second set of initial conditions.

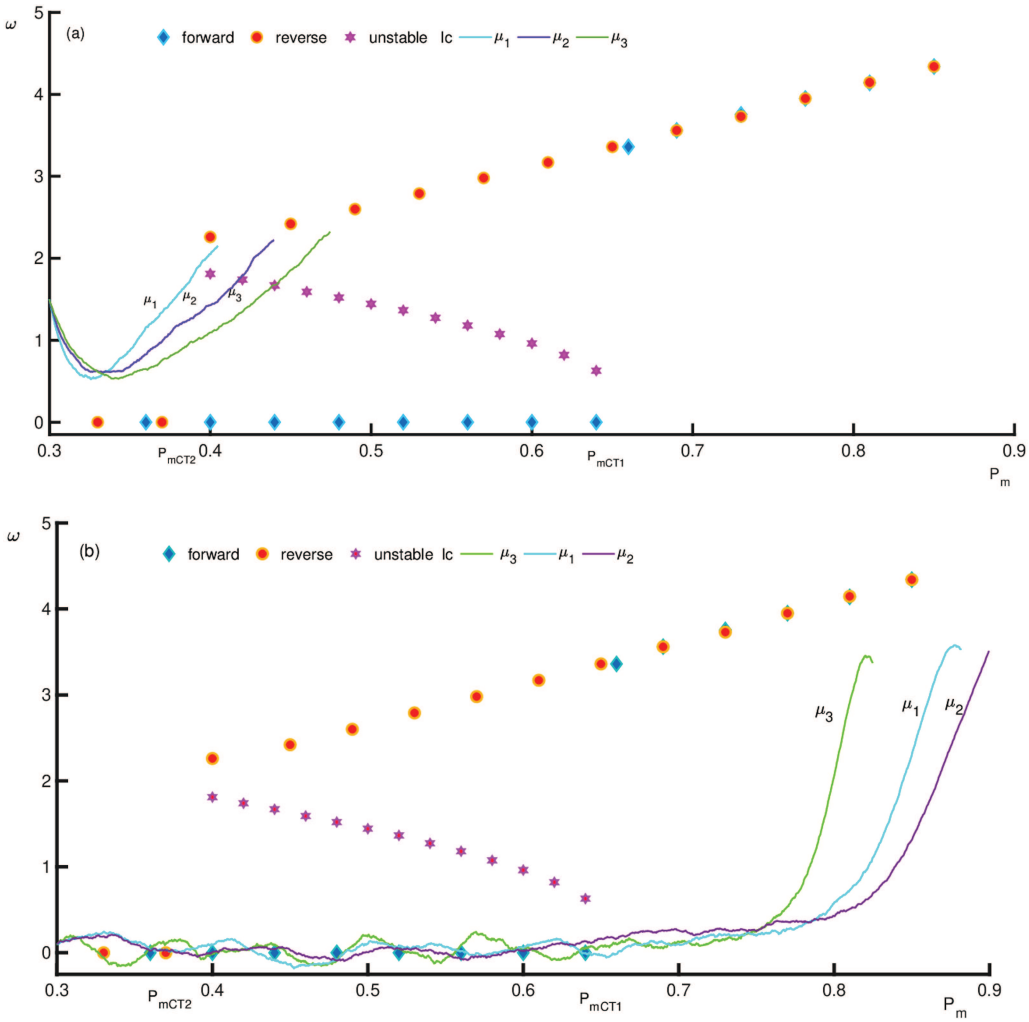

FIG. 1. Dependence of transition characteristics on the initial conditions. The figure depicts the trajectory of angular velocity for two different initial conditions with respect to the quasi-static bifurcation diagram. (a) Away from the fixed point: the initial condition is specified as follows: $\omega_0 = 1.5$, $P_{m0} = 0.3$. The mechanical power is allowed to vary at three different rates, as in the order $\mu_3 < \mu_2 < \mu_1$ at a noise intensity of $\sigma = 3\%$. (b) Near the fixed point: the initial condition is specified as follows: $\omega_0 = 0.1$, $P_{m0} = 0.3$. The mechanical power is allowed to vary at the same rate as in the earlier case with the same noise exposure. However, the order in which the transition occurs is not maintained, which is shown in the figure. The forward and backward paths of the quasi-static bifurcation diagram are indicated by blue and red colored markers, respectively.

Unlike the earlier case wherein the order of crossover is dependent upon respective μ, crossover depends upon the individual noise realization for the operating condition close to the fixed point.

Additionally, we captured multiple realizations of the response while maintaining the noise intensity, the rate of variation, and the initial conditions constant to check the variability in stochastic realization. As described earlier, we performed 50 simulations each for cases 1 and 2. We have plotted five realizations of the transitions corresponding to two different operating conditions, to ensure the clarity and to illustrate the spread in the point of transition, Case 1: $\mu = 0.0001$, $\omega_0 = 1.5$, $P_{mo} = 0.3$, $P_{mf} = 0.9$ and Case 2: $\mu = 0.0001$, $\omega_0 = 0.1$, $P_{mo} = 0.3$, $P_{mf} = 0.9$ when subjected to the same non-dimensional noise intensity of 3%. Figures 2(a) and 2(b) demonstrate the multiple realizations of the transitions pertaining to case 1 and 2, respectively. Our results are in qualitative agreement with the results observed by Unni *et al.* in thermoacoustic systems.[41]

The individual realizations of the trajectories exhibit substantial variability in the point of transition to limit cycle oscillations in the presence of noise in Fig. 2. We have computed the mean value of the transition point in both cases and computed the deviation in the transition point from the mean. This confirms the variability in the point of transition for each realization. We observe the variability in the transition point for multiple realizations in Fig. 2 with respect to Fig. 1. However, the pronounced effect of variability can be observed in the plot, corresponding to the second case [Fig. 2(b)], wherein the operating condition is close to the fixed point.

We infer that noise plays a crucial role in deciding the transition characteristic when the trajectory is near the fixed point. It is identified that pre-bifurcation noise amplification is pronounced

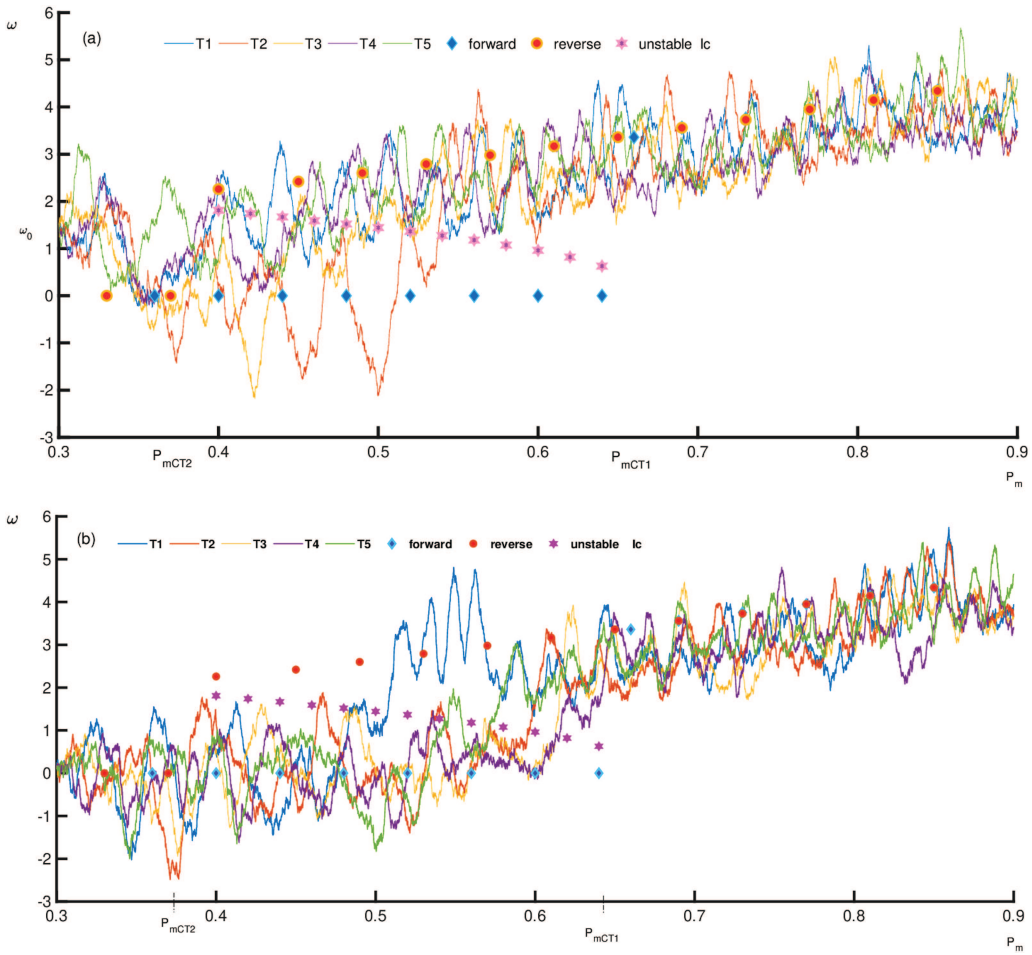

FIG. 2. Variable transition characteristics with respect to initial conditions and fluctuations. (a) Away from the fixed point, $\omega_0 = 1.5$. (b) Near the fixed point , $\omega_0 = 0.1$. Figures (a) and (b) depict the dynamic trajectories for the variation of mechanical power between P_{m0} and P_{mf}, respectively, at a prefixed rate and noise intensity. Here, the dynamic trajectories are marked as T1–T5 with respect to the quasi-static bifurcation diagram for the mechanical power variation from $P_{m0} = 0.3$ to $P_{mf} = 0.9$. The forward and backward paths of the quasi-static bifurcation diagram are indicated by blue and red colored markers, respectively. The pink colored hexagonal marks demarcates stable equilibrium point from the stable limit cycle.

for slow transitions through the bifurcation point in systems with internal noise.[40] In our study, we show that when the magnitudes of the operating state variables are comparable with the magnitudes of noise intensities, the system becomes stochastic. This is dissimilar to the expected behavior for the slow variation of system parameters through the bifurcation point.

Thus, we unveil that in the case of a stochastic bi-stable power system oscillator, there is an interplay between the noise and the rate, which determines the system response.

To identify the effects of noise intensity on the transition characteristics, we have repeated the experiments associated with Fig. 1 for various noise intensities for a given rate of variation of mechanical power (Fig. 3). We have considered 25 realizations of each noise intensity and computed the average trajectory to analyze the response in the presence of noise. We inferred that the dependence on initial conditions is preserved by inspecting the average trajectory of 25 realizations. We have observed complete suppression of the bi-stable region for noise intensity, $\sigma = 8\%$. Hence, in our study,

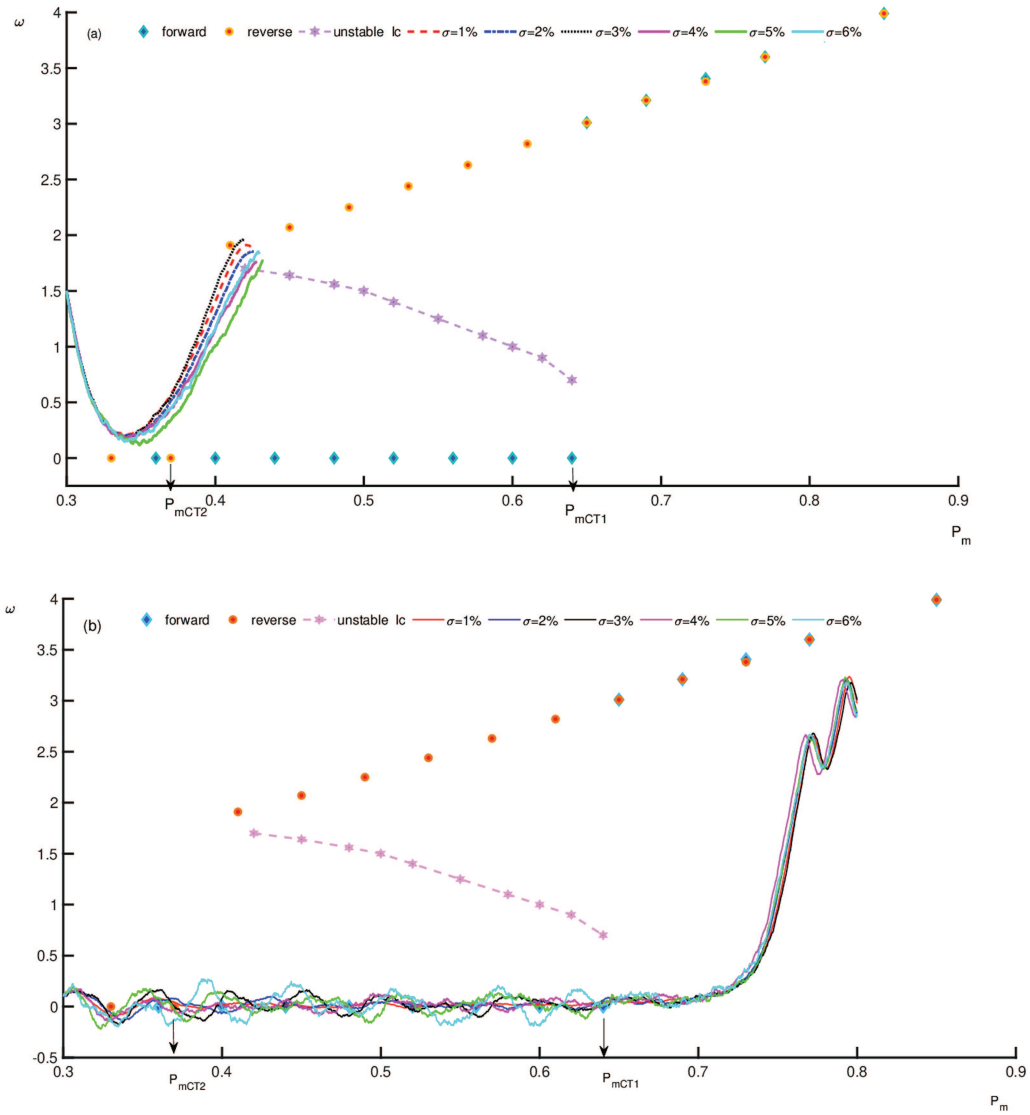

FIG. 3. Influence of noise intensity on the transition characteristics. The figure depicts the angular velocity for two different initial conditions when exposed to varying noise intensities with respect to the quasi-static bifurcation diagram. (a) Away from the fixed point. The initial conditions are the same as in Fig. 1 ($P_{m0} = 0.3, \omega_0 = 1.5$). The mechanical power is allowed to vary from 0.3 to 0.8 at a rate of $\mu = 0.0001$. The noise intensities considered in this experiment range from 1% to 6%. (b) Near the fixed point: the initial conditions are $\omega_0 = 0.1, P_{m0} = 0.3$ The average trajectory remains the same irrespective of the noise intensities considered.

to investigate the effect of noise intensity on the transitions, we consider noise intensities less than 8% to avoid the possibility of noise-induced transitions (NIT), which is beyond the scope of this work. There is a qualitative similarity between our results on the shift in the point of transition in the presence of fluctuations and the change in the bifurcation point observed in the Henon map[42] and loss-driven CO_2 laser.[43] We observe that the suppression of the bi-stable region for higher noise intensity (8%) is in qualitative agreement with the observation of the destabilization of the attractors by additive noise for the slow sinusoidal parameter variation in the logistic map[44] and annihilation of one of the coexisting attractors in a bistable system.[45]

We find that stochastic power systems show significant randomness at the point of transition, resulting in a loss of 80% of the stability margin determined by the quasi-static bifurcation diagram in the studies that we conducted. This leads to an emergency state, which necessitates a dedicated control strategy.[46–49] Therefore, it is extremely important to develop an effective control strategy for systems operating near to their physical limits, which is the subject of Sec. III B.

B. Rate-driven control of power system operating near the physical limits

The transition characteristics of stochastic power systems presented in Sec. III A. revealed that transitions are triggered by both noise and the operating environments. Power systems usually operate near the stability limits for the best usage of the existing transmission assets.[50] Therefore, stochastic power systems operating near the stability limits are more susceptible to the type of transitions that we observed in Sec. III A. We propose a control strategy for a stochastic power system operating close to the physical limits.

We consider a power system model that operates beyond the quasi-static bifurcation point to resemble a physical system operating close to the limits. In our previous experiments, we noticed that the power system exhibits a delay in transition when the control parameter varies as a function of time.[25] Here, we notice a small window from the point of transition to the point at which the trajectory grazes the limit cycle oscillations. The point of transition and the point at which the trajectory grazes the limit cycle oscillations are, respectively, shown as P_{tran} and P_{merg} in Fig. 4. Therefore, region of interest to develop a control scheme is from the bifurcation point, P_{mCT1}, to the merging point, P_{merg}, denoted as ΔP_m in Fig. 4. The time taken while traversing from P_{tran} to P_{merg} is dependent upon the rate at which the parameter is varied.

We vary the mechanical power from an initial value P_{m0} to a final value P_{mf} at a rate of $\mu = 0.0001$, the lowest rate considered for the experiment. Furthermore, we decremented the mechanical power at the same rate of the increment to check whether the decrement was sufficient to bring the system back to the basin of attraction of the fixed point. Initially, we choose a P_{mf} value close to P_{mCT1} in our numerical experiment. We incremented P_{mf} gradually in steps of 0.01 to identify the highest P_m for which the reverse transition to the stable fixed point is possible for $\mu = 0.0001$. We observed that for P_{mf} beyond 0.68, the angular velocity crosses the unstable limit cycle and enters the basin of attraction of the limit cycle, even though P_m is decremented at a rate of 0.0001. Figures 5(a) and 5(b) depict two representative cases from the numerical experiments conducted. In Fig. 5(a), the trajectory of ω crosses the unstable limit cycle, while we decrement the mechanical power for a P_{mf} value of 0.7. The crossover to the stable limit cycle is shown in green

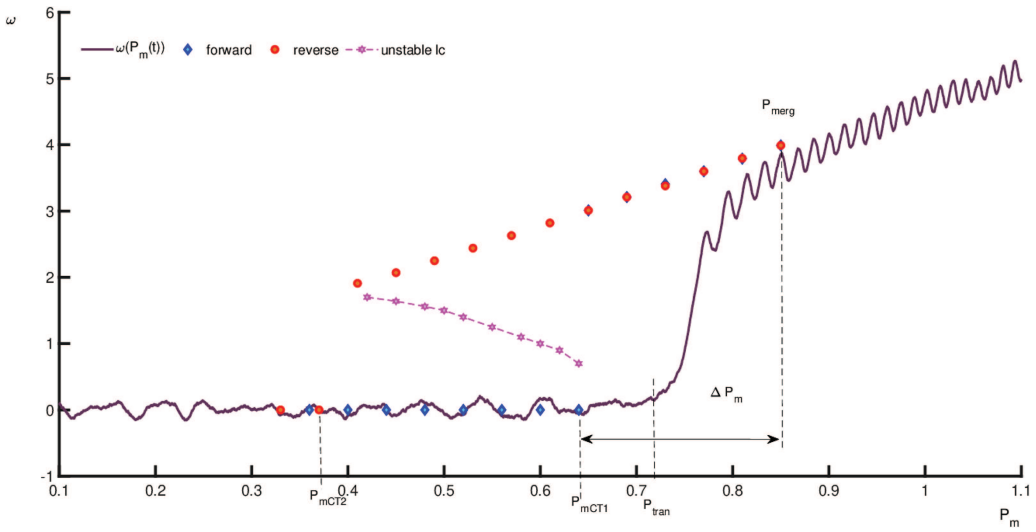

FIG. 4. Margin for control of the system for variations of mechanical power as a function of time. The figure shows the transition to the oscillatory state for the mechanical power variation as a function of time and the merging point with respect to the quasi-static bifurcation diagram for $\sigma = 3\%$. The transition and merging point is, respectively, denoted as P_{tran} and P_{merg}. The quasi-static bifurcation diagram is shown in blue and red colored markers for the forward and reverse paths, respectively. The window from the quasi-static bifurcation point Pm_{CT1} to merging point P_{merg} is marked as ΔP_m. The control parameter variation is performed at a rate of $\mu = 0.0001$.

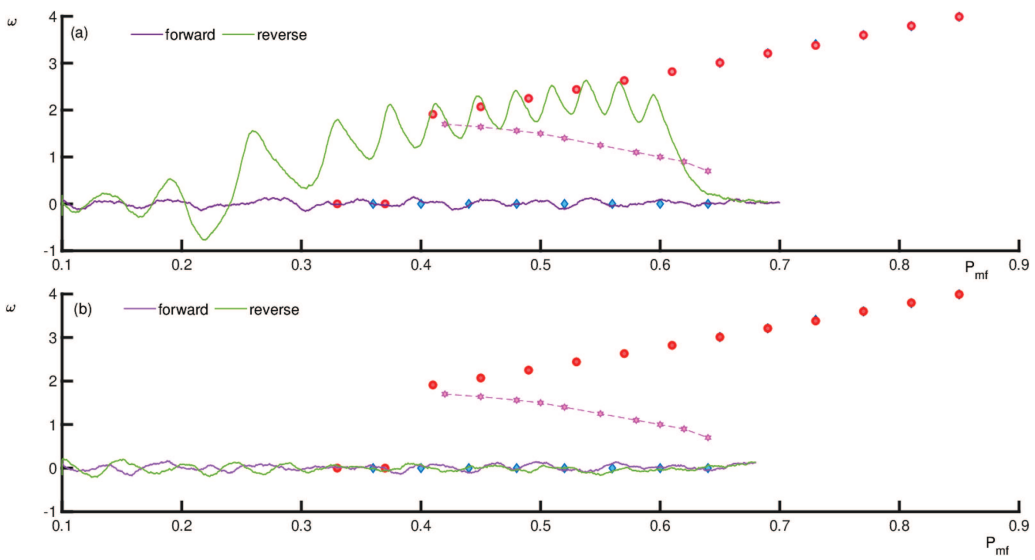

FIG. 5. The rate-driven control strategy. We vary the mechanical power at $\mu = 0.0001$ from $P_{m0} = 0.1$ to P_{mf} and decrement from P_{mf} at the same rate for $\sigma = 3\%$. The response of the system for the increment and decrement of P_m is shown by blue and red colored trajectories against the bifurcation diagram. In Fig. 5(a), $P_{mf} = 0.7$, where we can observe the transition to the stable oscillatory state, despite the decrement in P_m. Figure 5(b) $P_{mf} = 0.68$, where the system regains the stable non-oscillatory state via the control strategy.

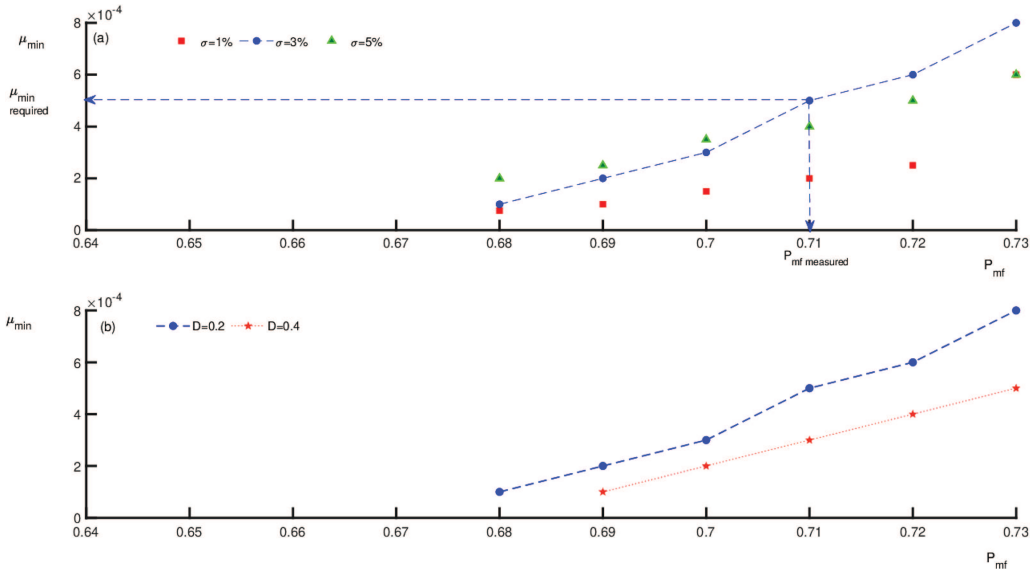

FIG. 6. Calibration curve is a plot, which shows the rate of the decrement of mechanical power (μ) required to perform a smooth reverse transition of the power system from the emergency regime to the stable regime for $\sigma = 1\%$, $\sigma = 3\%$, and $\sigma = 5\%$, respectively. Figure 6(a) shows the calibration curve that illustrates the minimum rate required to revert the system back to stable non-oscillatory state for different P_{mf} values, when $D = 0.2$. Figure 6(b) shows the comparison of the minimum rate required for the decrement of mechanical power for two damping values. The figure depicts the reduction in the value of μ_{min} for an increase in damping performed at a noise intensity of 3%.

colored trajectory in Fig. 5(a). In the latter case, ω returns to the basin of attraction of fixed point [Fig. 5(b)] when P_{mf} is decremented to 0.68.

Next, we performed the numerical experiment to determine the maximum P_m, which allows the reversal of transition by incrementing μ values while decreasing the mechanical power for three different noise intensities. We focus on the region between the quasi-static bifurcation point (P_{mCT1}) to the merging point (P_{merg}) to determine the μ_{min} of the model that operates around the stability margin. We show the results in the calibration curve in Fig. 6(a), which illustrates the minimum rate of the decrement of the mechanical power, μ_{min}, to perform a smooth reversal from the emergency state to the regime of safe return, for three different noise intensities, 1%, 3%, and 5%, respectively. We can ensure stability by operating at mechanical power decrements between μ_{min} and the maximum limit imposed by the physical constraints.

Furthermore, we captured multiple realizations of the response for a predetermined μ_{min} and a given noise intensity (σ) to check the variability in the stochastic realization. We performed the experiment for all the noise intensities considered in the calibration curve. By analyzing the results, we observed that there exists variability in μ_{min} among multiple realizations of the same noise intensity. In an attempt to extend the P_{mf} value, we incremented the damping level of the system. We identified that it is possible to ensure a safe return to the non-oscillatory state with a lower rate of decrement of mechanical power by increasing the damping level of the system [Fig. 6(b)]. In Fig. 6, the recommended region for operation pertaining to P_{mf} is above the blue and red trajectories for $D1$ and $D2$, respectively. From the numerical experiments, we observe that if we perform the forward transition at $\mu = 0.0001$, there exists an upper limit for P_{mf}, beyond which the reverse transition to the stable fixed point will not be possible.

The proposed rate-driven control strategy for emergency control based on universal bifurcation regularity implies a practical application in different fields where a reverse transition from an unstable to a stable state is needed. The proposed rate-driven control strategy helps maintain the stability of engineering systems such as power systems,[26] thermoacoustic systems,[41] and in agroecological transitions[51,52] when the systems are operating near the physical limits.

IV. CONCLUSIONS

This paper focuses on the role of the initial conditions and the stochastic fluctuations in the onset of oscillations in a bi-stable power system model that undergoes rate-dependent variation of the control parameter, which has not been investigated in power systems.

Our first finding is that when the magnitudes of the noise intensity and the state variable are comparable, the system undergoes noise-induced transitions while crossing the unstable limit cycle. In these noise-induced transitions, the effect of rate on the transition characteristics is diminished and the system response is purely determined by the noise level present in the system. This is dissimilar to the expected behavior in systems that undergo a slow passage through the bifurcation.

Second, we estimate the variability in the operating margin for a given noise intensity and the rate of variation of the control parameter for different initial conditions.

Our most striking result is a safe-return control strategy from the emergency state to the stable regime. We established a boundary between the emergency state and regime of safe return in the plane of mechanical power limit and the rate of decrement of mechanical power.

The proposed emergency control strategy helps retain stability by deciding the rate of the decrement of the control parameter for operation beyond the bifurcation point by modifying the generation of redispatch. Furthermore, we find that the relation between the damping constant and the rate plays a significant role in deciding the energy sources to be retained while operating near the stability limits. We propose to analyze the effect of the effectiveness of the control strategy in a real-time power grid where inherent noise will be there as future work.

ACKNOWLEDGMENTS

K.S.S. gratefully acknowledges the financial support provided by Amrita Vishwa Vidyapeetham and the valuable suggestions and comments in the manuscript preparation given by Professor Sudha Balagopalan. J.K. thanks the financial support of the EPICC project (18-II-149-Global-A-Risikovorhersage) funded by the BMU. E.S. acknowledges the financial support of the Russian Foundation for Basic Research (RFBR) (No. 20-07-01071).

AUTHOR DECLARATIONS

Conflict of Interest

The authors have no conflicts to disclose.

DATA AVAILABILITY

The data that support the findings of this study are available from the corresponding author upon reasonable request.

REFERENCES

[1] P. Ju, H. Li, X. Pan, C. Gan, Y. Liu, and Y. Liu, "Stochastic dynamic analysis for power systems under uncertain variability," IEEE Trans. Power Syst. **33**(4), 3789–3799 (2017).
[2] Y. V. Makarov, P. V. Etingov, J. Ma, Z. Huang, and K. Subbarao, "Incorporating uncertainty of wind power generation forecast into power system operation, dispatch, and unit commitment procedures," IEEE Trans. Sustainable Energy **2**(4), 433–442 (2011).
[3] C. Wang, L. Shi, L. Yao, L. Wang, Y. Ni, and M. Bazargan, "Modelling analysis in power system small signal stability considering uncertainty of wind generation," in *IEEE PES General Meeting* (IEEE, 2010), pp. 1–7.
[4] S. M. Shahidehpour and J. Qiu, "Effect of random perturbations on the dynamic behavior of power systems," Electr. Power Syst. Res. **11**(2), 117–127 (1986).
[5] R. M. Hassan and C. O. Nwankpa, "A stochastic model for power system transformer tap-changers," in *1992 American Control Conference* (IEEE, 1992), pp. 1732–1733.
[6] M. Olsson, M. Perninge, and L. Söder, "Modeling real-time balancing power demands in wind power systems using stochastic differential equations," Electr. Power Syst. Res. **80**(8), 966–974 (2010).
[7] R. Calif, "PDF models and synthetic model for the wind speed fluctuations based on the resolution of Langevin equation," Appl. Energy **99**, 173–182 (2012).

[8]Y. Xu, F. Wen, H. Zhao, M. Chen, Z. Yang, and H. Shang, "Stochastic small signal stability of a power system with uncertainties," Energies **11**(11), 2980 (2018).
[9]A. S. Pikovsky and J. Kurths, "Coherence resonance in a noise-driven excitable system," Phys. Rev. Lett. **78**(5), 775 (1997).
[10]O. V. Ushakov, H.-J. Wünsche, F. Henneberger, I. A. Khovanov, L. Schimansky-Geier, and M. A. Zaks, "Coherence resonance near a Hopf bifurcation," Phys. Rev. Lett. **95**(12), 123903 (2005).
[11]I. Bashkirtseva, T. Ryazanova, and L. Ryashko, "Stochastic bifurcations caused by multiplicative noise in systems with hard excitement of auto-oscillations," Phys. Rev. E **92**(4), 042908 (2015).
[12]C. O. Nwankpa, S. M. Shahidehpour, and Z. Schuss, "A stochastic approach to small disturbance stability analysis," IEEE Trans. Power Syst. **7**(4), 1519–1528 (1992).
[13]J. R. Hockenberry and B. C. Lesieutre, "Evaluation of uncertainty in dynamic simulations of power system models: The probabilistic collocation method," IEEE Trans. Power Syst. **19**(3), 1483–1491 (2004).
[14]P. Kundur, *Power System Stability and Control* (McGraw Hill, New York, 2007).
[15]C. De Marco and A. Bergen, "A security measure for random load disturbances in nonlinear power system models," IEEE Trans. Circuits Syst. **34**(12), 1546–1557 (1987).
[16]K. Wang and M. L. Crow, "The Fokker–Planck equation for power system stability probability density function evolution," IEEE Trans. Power Syst. **28**(3), 2994–3001 (2013).
[17]G. Ghanavati, P. D. H. Hines, T. I. Lakoba, and E. Cotilla-Sanchez, "Understanding early indicators of critical transitions in power systems from autocorrelation functions," IEEE Trans. Circuits Syst. I: Reg. Pap. **61**(9), 2747–2760 (2014).
[18]Z. Y. Dong, J. H. Zhao, and D. J. Hill, "Numerical simulation for stochastic transient stability assessment," IEEE Trans. Power Syst. **27**(4), 1741–1749 (2012).
[19]F. Milano and R. Zárate-Miñano, "A systematic method to model power systems as stochastic differential algebraic equations," IEEE Trans. Power Syst. **28**(4), 4537–4544 (2013).
[20]T. Odun-Ayo and M. L. Crow, "Structure-preserved power system transient stability using stochastic energy functions," IEEE Trans. Power Syst. **27**(3), 1450–1458 (2012).
[21]S. V. Dhople, Yu. C. Chen, L. DeVille, and A. D. Domínguez-García, "Analysis of power system dynamics subject to stochastic power injections," IEEE Trans. Circuits Syst. I: Reg. Pap. **60**(12), 3341–3353 (2013).
[22]K. Wang and M. L. Crow, "Investigation on singularity of stochastic differential algebraic power system model," in *2011 North American Power Symposium* (IEEE, 2011), pp. 1–5.
[23]S. M. Baer, T. Erneux, and J. Rinzel, "The slow passage through a Hopf bifurcation: Delay, memory effects, and resonance," SIAM J. Appl. Math. **49**(1), 55–71 (1989).
[24]J. Tony, S. Subarna, K. S. Syamkumar, G. Sudha, S. Akshay, E. A. Gopalakrishnan, E. Surovyatkina, and R. I. Sujith, "Experimental investigation on preconditioned rate induced tipping in a thermoacoustic system," Sci. Rep. **7**(1), 5414 (2017).
[25]K. S. Suchithra and E. A. Gopalakrishnan, "Rate dependent transitions in power systems," in *2018 International Conference and Utility Exhibition on Green Energy for Sustainable Development (ICUE)* (IEEE, 2018), pp. 1–5.
[26]K. S. Suchithra, E. A. Gopalakrishnan, E. Surovyatkina, and J. Kurths, "Rate-induced transitions and advanced takeoff in power systems," Chaos **30**(6), 061103 (2020).
[27]A. Majumdar, J. Ockendon, P. Howell, and E. Surovyatkina, "Transitions through critical temperatures in nematic liquid crystals," Phys. Rev. E **88**(2), 022501 (2013).
[28]J. Ma, Y. Sun, X. Yuan, J. Kurths, and M. Zhan, "Dynamics and collapse in a power system model with voltage variation: The damping effect," PLoS One **11**(11), e0165943 (2016).
[29]W. Ji and V. Venkatasubramanian, "Hard-limit induced chaos in a single-machine-infinite-bus power system," in *Proceedings of 1995 34th IEEE Conference on Decision and Control* (IEEE, 1995), Vol. 4, pp. 3465–3470.
[30]K. Schmietendorf, J. Peinke, and O. Kamps, "On the stability and quality of power grids subjected to intermittent feed-in," arXiv:1611.08235.
[31]S. Auer, F. Hellmann, M. Krause, and J. Kurths, "Stability of synchrony against local intermittent fluctuations in tree-like power grids," Chaos **27**(12), 127003 (2017).
[32]B. Yuan, M. Zhou, G. Li, and X.-P. Zhang, "Stochastic small-signal stability of power systems with wind power generation," IEEE Trans. Power Syst. **30**(4), 1680–1689 (2014).
[33]R. L. Honeycutt, "Stochastic Runge–Kutta algorithms. I. White noise," Phys. Rev. A **45**(2), 600 (1992).
[34]V. Ajjarapu and B. Lee, "Bifurcation theory and its application to nonlinear dynamical phenomena in an electrical power system," IEEE Trans. Power Syst. **7**(1), 424–431 (1992).
[35]G. Pierrou and X. Wang, "Analytical study of the impacts of stochastic load fluctuation on the dynamic voltage stability margin using bifurcation theory," IEEE Trans. Circuits Syst. I: Reg. Pap. **67**(4), 1286–1295 (2019).
[36]J. Cidras and A. E. Feijoo, "A linear dynamic model for asynchronous wind turbines with mechanical fluctuations," IEEE Trans. Power Syst. **17**(3), 681–687 (2002).
[37]E. A. Gopalakrishnan and R. I. Sujith, "Effect of external noise on the hysteresis characteristics of a thermoacoustic system," J. Fluid Mech. **776**, 334–353 (2015).
[38]P. G. Meyer, M. Anvari, and H. Kantz, "Identifying characteristic time scales in power grid frequency fluctuations with DFA," Chaos **30**(1), 013130 (2020).
[39]M. Anvari, L. R. Gorjão, M. Timme, D. Witthaut, B. Schäfer, and H. Kantz, "Stochastic properties of the frequency dynamics in real and synthetic power grids," Phys. Rev. Res. **2**(1), 013339 (2020).
[40]E. D. Surovyatkina, Yu. A. Kravtsov, and J. Kurths, "Fluctuation growth and saturation in nonlinear oscillators on the threshold of bifurcation of spontaneous symmetry breaking," Phys. Rev. E **72**(4), 046125 (2005).
[41]V. R. Unni, E. A. Gopalakrishnan, K. S. Syamkumar, R. I. Sujith, E. Surovyatkina, and J. Kurths, "Interplay between random fluctuations and rate dependent phenomena at slow passage to limit-cycle oscillations in a bistable thermoacoustic system," Chaos **29**(3), 031102 (2019).
[42]J. M. Saucedo-Solorio, A. N. Pisarchik, and V. Aboites, "Shift of critical points in the parametrically modulated hénon map with coexisting attractors," Phys. Lett. A **304**(1–2), 21–29 (2002).
[43]A. N. Pisarchik and R. Corbalán, "Shift of attractor boundaries in a system with a slow harmonic parameter perturbation," Phys. D **150**(1–2), 14–24 (2001).
[44]H. G. Davies and K. Rangavajhula, "A period-doubling bifurcation with slow parametric variation and additive noise," Proc. R. Soc. London, Ser. A **457**(2016), 2965–2982 (2001).
[45]A. N. Pisarchik and B. K. Goswami, "Annihilation of one of the coexisting attractors in a bistable system," Phys. Rev. Lett. **84**(7), 1423 (2000).
[46]P. Kundur and G. K. Morison, "Techniques for emergency control of power systems and their implementation," IFAC Proc. Vol. **30**(17), 639–644 (1997).
[47]A. N. Pisarchik, "Dynamical tracking of unstable periodic orbits," Phys. Lett. A **242**(3), 152–162 (1998).
[48]B. E. Martínez-Zerega, A. N. Pisarchik, and L. S. Tsimring, "Using periodic modulation to control coexisting attractors induced by delayed feedback," Phys. Lett. A **318**(1–2), 102–111 (2003).
[49]A. N. Pisarchik and U. Feudel, "Control of multistability," Phys. Rep. **540**(4), 167–218 (2014).
[50]J. W. Simpson-Porco, F. Dörfler, and F. Bullo, "Voltage collapse in complex power grids," Nat. Commun. **7**(1), 1–8 (2016).
[51]G. Ollivier, D. Magda, A. Mazé, G. Plumecocq, and C. Lamine, "Agroecological transitions: What can sustainability transition frameworks teach us? An ontological and empirical analysis," Ecol. Soc. **23**(2), 18 (2018).
[52]E. Sachet, O. Mertz, J.-F. Le Coq, G. S. Cruz-Garcia, W. Francesconi, M. Bonin, and M. Quintero, "Agroecological transitions: A systematic review of research approaches and prospects for participatory action methods," Front. Sustain. Food Syst. **5**, 397 (2021).